

UDC 548.736.442.6:546.42/733/723/882

Investigation of the Functional Characteristics of Perovskites $\text{SrCo}_{0.8-x}\text{Fe}_{0.2}\text{Nb}_x\text{O}_{3-z}$

A. S. KOZHEMYACHENKO and A. P. NEMUDRY

*Institute of Solid State Chemistry and Mechanochemistry, Siberian Branch of the Russian Academy of Sciences, Ul. Kutateladze 18, Novosibirsk 6300128 (Russia)**E-mail: nemudry@solid.nsc.ru*

(Received January 21, 2010; revised March 10, 2010)

Abstract

Single-phase membrane materials having the composition $\text{SrCo}_{0.8-x}\text{Nb}_x\text{Fe}_{0.2}\text{O}_{3-z}$ were obtained. The effect of doping with niobium on thermal stability and transport characteristics of the obtained compounds was studied. It was shown that the isomorphous substitution of cobalt ions with highly charged Nb^{5+} cations causes an increase in thermal stability of the compounds under investigation in the reductive atmosphere and suppression of the phase transition perovskite – brownmillerite, which is accompanied by acceptable decrease in oxygen permeability.

Key words: perovskites, oxygen-permeable membranes, thermochemical stability, electrochemical oxidation, oxygen transport

INTRODUCTION

Synthesis gas is essential intermediate product of chemical industry used for the synthesis of ammonia and methanol, and also as a source of hydrogen. At present synthesis gas is obtained by means of steam conversion of methane. This process is power consuming. It is more profitable to obtain synthesis gas through the partial oxidation of methane but pure oxygen is necessary for this reaction. Cryogenic purification of oxygen is an expensive process, so attention of researchers has been attracted during the recent years to the development of membranes for oxygen separation from the air. Oxidation of methane into synthesis gas on the surface of a gas-tight membrane with mixed electronic conductivity is more efficient because the processes of oxygen separation and partial oxidation of methane are brought together in the reactor which is relatively simple in design. However, the material of the membrane should meet a number of requirements: it must possess high oxygen permeability (0.1–1 mmol/($\text{cm}^2 \cdot \text{s}$) at $T > 800$ °C), chemical stability in reductive and oxidative atmospheres and thermal

expansion coefficients within the range 16–20 10^{-1}K^{-1} [1].

Promising materials for oxygen-permeable membranes are mixed electron-ionic conductors with perovskite structure. It is known that $\text{SrCo}_{0.8}\text{Fe}_{0.2}\text{O}_{3-z}$ possesses high oxygen permeability [2, 3] but this compound is unstable in the reducing atmosphere. Also a decrease in the partial pressure of oxygen above the sample causes phase transition perovskite–brownmillerite [4]. This process is accompanied by the change of volume, which can cause the destruction of the membrane. In addition, the formation of brownmillerite structure is accompanied by ordering of oxygen vacancies, their localization and, as a consequence, a sharp decrease of oxygen mobility.

One of the efficient methods to modify the properties of materials is doping. Perovskite ABO_{3-x} structure possesses high tolerance to substitutions, which allows one to vary functional properties of perovskite-like oxides within a broad range. A large number of works considered substitutions either in A sublattice or in B. As a rule, substitution of Sr for La, Ba and other alkaline-earth and rare-earth cations

occurs in A sublattice. Mainly isovalent substitutions are used in B sublattice (Al, Ga, Ni, Cu, Cr, Ti *etc.*) [5–8]. Introduction of cations M^{3+} into the structure of perovskites based on strontium cobaltite and ferrite allows one to conserve high concentration of oxygen vacancies but increases the probability of their ordering and leads to a decrease in oxygen conductance [9]. Selection of various doping additives with stable oxidation degree (Al, Ga *etc.*) allows one to increase thermal stability and decrease the value of the chemical component of CTE [10–12].

Previously we proposed to use cations with high oxidation degree (Mo^{6+} , W^{6+} , Nb^{5+} , Ta^{5+}) as dopants [13–16]. Doping with highly charged cations causes an increase in oxygen content in the oxide and thus brings the system out of the stability region of ordered brownmillerite phase at low partial pressures of oxygen $AB_{1-x}M_xO_{2.5+z}$. The formation of strong MO_6 octahedrons increases thermochemical stability of materials. In addition, we demonstrated in [12, 13] that the substitution of 5 at. % Fe for Mo in strontium ferrite causes an increase in oxygen conductance in comparison with the initial $SrFeO_{3-x}$.

Ions Mo^{6+} , W^{6+} , Nb^{5+} , Ta^{5+} are interesting as ferroelectric cations promoting in particular the appearance of ferroelastic properties of materials [18]. As a result, the introduction of niobium ions into the lattice of $SrCo_{0.8}Fe_{0.2}O_{3-z}$ is accompanied by nanostructuring effects [19] – twinning of the crystals of substituted perovskites at the nanometer level and the formation of the high density of twin boundaries that may serve as the channels of facilitated diffusion of oxygen ions [20, 21].

The goal of the present work was to study the system $SrCo_{0.8}Fe_{0.2}O_{3-z}$ doped with niobium ions, and the effect of substitutions in B sublattice on the functional properties of materials $SrCo_{0.8-x}Fe_{0.2}Nb_xO_{3-z}$ (thermochemical stability, oxygen mobility at room temperature, oxygen permeability at high temperatures).

EXPERIMENTAL

The samples were synthesized using the standard ceramic method described previously in [16], from corresponding oxides and carbonates

of metals at the synthesis temperature within the range 1250–1450 °C. Different kinds of sample treatment were used to change the oxygen stoichiometry: cooling in the furnace, annealing of the furnace-cooled samples in a quartz ampoule at 950 °C in the dynamic vacuum ($P \sim 10$ Pa) followed by quenching of the samples to room temperature. Oxygen content in the synthesized samples was determined by iodometric titration. XPA was carried out using a DRON-3 diffractometer (CuK_{α} radiation). Thermal stability of slowly cooled samples in the reductive atmosphere (5 % H_2 + 95 % Ar) was studied using a Netzsch STA 449C Jupiter derivatograph. Oxygen mobility at room temperature was estimated on the basis of the electrochemical oxidation of samples quenched in vacuum in the galvanostatic mode [22].

Oxygen mobility at high temperature was measured in a model membrane reactor de-

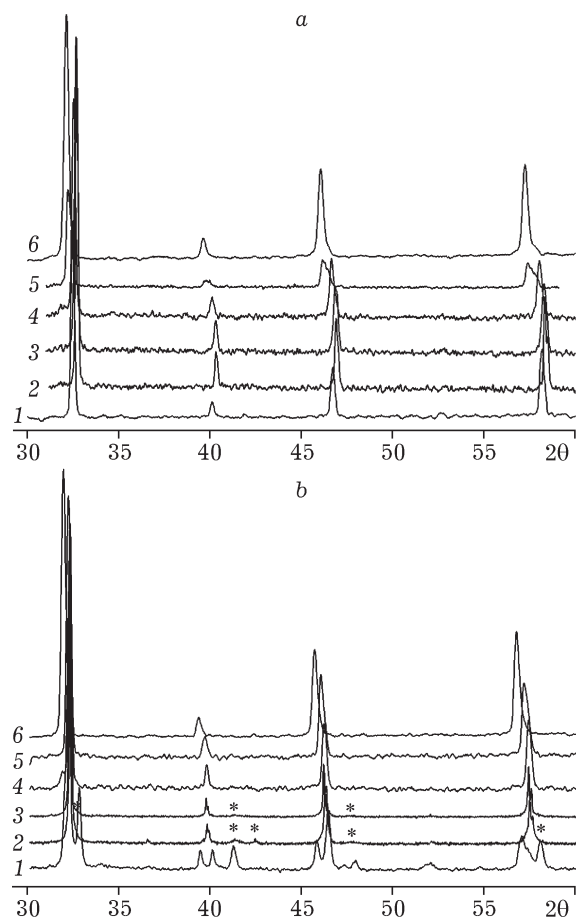


Fig. 1. X-ray diffraction patterns of the samples doped with niobium: *a* – slowly cooled in the air; *b* – quenched in vacuum; niobium content x : 0 (1), 0.05 (2), 0.1 (3), 0.2 (4), 0.3 (5), 0.4 (6).

TABLE 1

 Structural parameters and oxygen content (z) for treated samples $\text{SrCo}_{0.8-x}\text{Fe}_{0.2}\text{Nb}_x\text{O}_z$

Niobium content (x)	Slowly cooled		Quenched in vacuum	
	a , Å	z	a , Å	z
0	3.848(2)	2.64	$a = 5.469(1)$ $b = 15.86(3)$ $c = 5.606(1)$	2.43
0.05	3.873(1)	2.74	$a = 5.552(1)$ $b = 15.80(1)$ $c = 5.544(2)$	2.47
0.1	3.877(1)	2.79	$a = 5.556(1)$ $c = 15.79(1)$	2.52
0.2	3.893(1)	2.81	3.935(1)	2.64
0.3	3.926(1)	2.88	3.948(1)	2.72
0.4	3.943(2)	2.94	3.981(2)	2.81

scribed in [23]. Gas-tight disc (density: about 95 %) made of the material under investigation, 15–17 mm in diameter and 1.2–1.5 mm thick, was tightly sealed with the help of glass liners into a cell. The sample was blown with the air from the external side, with the flow rate of 100 mL/min. Argon or helium was blown over the inner side with the flow rate of 5–70 mL/min. Measurements of oxygen permeability were performed within temperature range 750–950 °C on a QMS 200 gas analyzer.

RESULTS AND DISCUSSION

X-ray diffraction patterns of the synthesized samples slowly cooled in the air are shown in Fig. 1, *a*. According to the XPA data, the synthesis leads to the formation of monophasic products having the cubic perovskite structure $Pm\bar{3}m$. Unit cell parameters and the data on oxygen content for slowly cooled and vacuum-quenched samples are shown in Table 1. Unit cell parameters increase monotonously with an increase in dopant content, which is the evidence of its isomorphous insertion into the structure. Fig. 1, *b* shows the diffraction patterns of the samples exposed and quenched in vacuum. The sample with $x = 0$ (curve 1) has brownmillerite structure; the X-ray diffraction pattern is indexed in the rhombic cell. The X-ray diffraction patterns of the samples with $x = 0.05$ and 0.1 (curves 2 and 3, respectively)

contain additional reflections marked with asterisk. The pattern of the sample with $x = 0.05$ can be indicated in the rhombic cell, while that with $x = 0.01$ can be indicated in the tetragonal cell. For niobium content 20 at. % and more, the cubic structure is conserved during quenching in vacuum.

Thus, the introduction of niobium in the amount of more than 10 at. % leads to an increase in oxygen content of the sample and narrowing of the interval of oxygen nonstoichiometry, which brings the system out of the region of stability of brownmillerite structure.

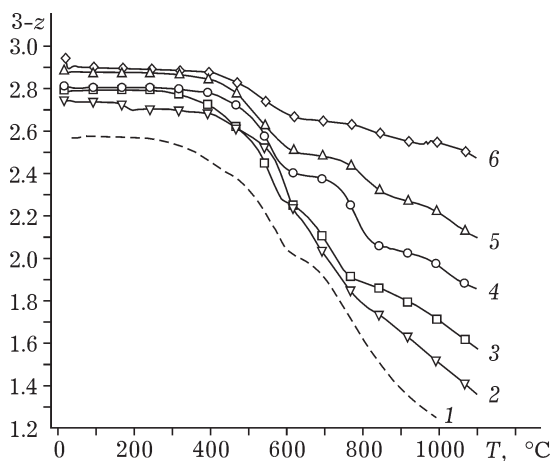


Fig. 2. Data of thermogravimetry for slowly cooled $\text{SrCo}_{0.8-x}\text{Fe}_{0.2}\text{Nb}_x\text{O}_{3-z}$ samples in the atmosphere of 5 % H_2 + 95 % Ar (heating rate: 10 K/min): 1 – initial $\text{SrCo}_{0.8}\text{Fe}_{0.2}\text{O}_{3-z}$, 2–6 – niobium content 5, 10, 20, 30, 40 %, respectively.

The results of the investigation of thermochemical stability of slowly cooled samples with different niobium content by means of thermogravimetry are presented in Fig. 2. One can see that the initial sample $\text{SrCo}_{0.8}\text{Fe}_{0.2}\text{O}_{3-z}$ heated in the atmosphere of 5% H_2 + 95% Ar starts to lose oxygen at $T = 200$ °C. Flexure on the curve of mass loss in the region of $T \sim 410$ °C corresponds to the formation of brownmillerite having the composition $\text{SrCo}_{0.8}\text{Fe}_{0.2}\text{O}_{2.43}$. A plateau at $T \sim 650$ °C corresponds to a complete reduction of ions $\text{Co}^{3+} \rightarrow \text{Co}^{2+}$ and apparently to the formation of Ruddlesden–Popper phases having the composition $\text{AO} \cdot (\text{ABO}_3)_n$. Subsequent heating causes the reduction of ions $\text{Co}^{2+} \rightarrow \text{Co}^0$ and later on leads to the formation of metal iron. The substitution of Co by 5 and 10 at. % niobium causes an increase in the stability limit of brownmillerite structure to $T \sim 550$ and 600 °C, respectively. With further increase in niobium content, the plateau corresponding to oxidation degrees Co^{2+} and Fe^{3+} and the region of stability of perovskite-like structures becomes more clearly pronounced.

So, with an increase in niobium content the maximal temperature of degradation of perovskite-like membrane materials increases from 650 to 800 °C.

Phase transformations at a temperature of 600–800 °C were studied with the composition $\text{SrCo}_{0.6}\text{Fe}_{0.2}\text{Nb}_{0.2}\text{O}_{3-z}$ with the help of *in situ* X-ray diffraction. For this purpose, slowly cooled samples were kept at different temperatures in the atmosphere of 5% H_2/Ar for 1 h, cooled to room temperature in the same atmosphere, then X-ray diffraction patterns were recorded (Fig. 3). One can see that the perovskite structure is conserved up to $T \sim 600$ °C, and afterwards the Ruddlesden–Popper phases are formed as more stable under these conditions [15], and metal cobalt, according to equation

$$10\text{SrCo}_{0.6}\text{Fe}_{0.2}\text{Nb}_{0.2}\text{O}_{2.4} + 4\text{H}_2 = 5\text{Sr}_2\text{Co}_{0.2}\text{Fe}_{0.4}\text{Nb}_{0.4}\text{O}_4 + 5\text{Co} + 4\text{H}_2\text{O} \quad (1)$$

As demonstrated previously [16], room-temperature electrochemical oxidation of nonstoichiometric perovskites based on strontium cobaltites and ferrites allows one to obtain the information about phase transitions accompanying the changes of oxygen stoichiometry and to estimate the coefficients of oxygen diffusion.

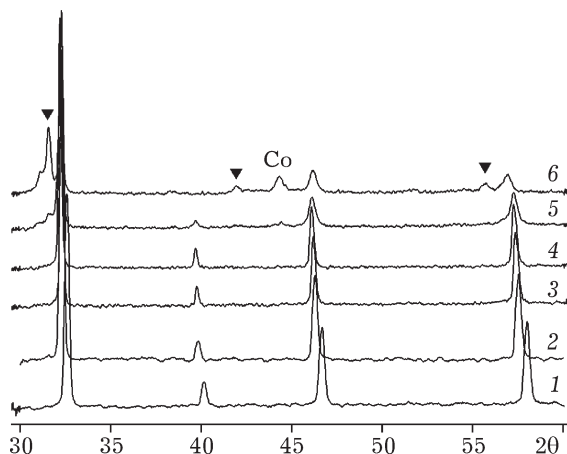
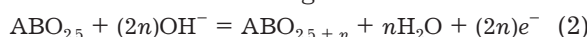


Fig. 3. Results of *ex situ* X-ray phase studies of $\text{SrCo}_{0.6}\text{Fe}_{0.2}\text{Nb}_{0.2}\text{O}_{3-z}$ samples: 1 – slowly cooled, 2 – quenched in vacuum, 3–6 – kept in the atmosphere of 5% H_2 + 95% Ar at 500, 600, 700, 800 °C, respectively; black triangle marks the reflections corresponding to Ruddlesden–Popper phase.

While the current passes through the cell containing alkali solution, the process taking place on the sample serving as the anode involves oxygen intercalation into the structure of the substance under investigation:



In the absence of side reactions, the transferred charge is linked with the amount of intercalated oxygen through equation

$$\delta = QM/zFm$$

where Q is transferred charge; M is molar mass; m is sample mass; F is Faraday constant; z is particle charge ($z = 2$ for oxide ions). Oxygen intercalation into the sample as a result of redox topotaxial reaction causes changes of its potential, and the resulting curves of potential *versus* transferred charge allow one to speak of phase transformations in samples during electrochemical oxidation. A monotonous change of potential provides evidence of single-phase oxidation mechanism, and the occurrence of a plateau corresponds to the oxidation in the two-phase mode. Thus, there are two plateaus on the curve of $\text{SrCo}_{0.8}\text{Fe}_{0.2}\text{O}_{3-z}$ oxidation: the first one corresponds to phase transition from $\text{SrCo}_{0.8}\text{Fe}_{0.2}\text{O}_{2.5}$ into $\text{SrCo}_{0.8}\text{Fe}_{0.2}\text{O}_{2.75}$, while the second relates to the phase transition from $\text{SrCo}_{0.8}\text{Fe}_{0.2}\text{O}_{2.75}$ into $\text{SrCo}_{0.8}\text{Fe}_{0.2}\text{O}_{2.87}$. The potential reaches the plateau at $E \sim 500$ mV, which is connected with the maximal oxidation of the

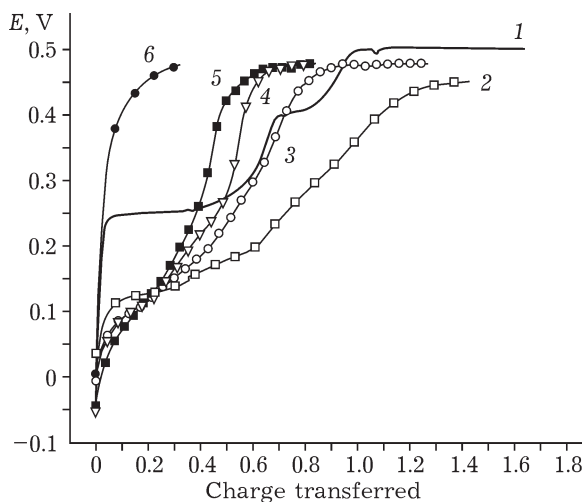
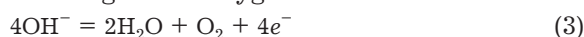


Fig. 4. Curves potential-transferred charge obtained during electrochemical oxidation of vacuum-quenched samples having composition $\text{SrCo}_{0.8-x}\text{Fe}_{0.2}\text{Nb}_x\text{O}_{3-z}$ ($y = 0-0.4$) in the galvanostatic mode in 1 M KOH solution. The values of x : 0 (1), 0.05 (2), 0.1 (3), 0.2 (4), 0.3 (5), 0.4 (6).

sample to $\text{SrCo}_{0.8}\text{Fe}_{0.2}\text{O}_{3.0}$ [22]. Further current passing through the cell does not cause any changes of the potential and is connected with the oxidation of hydroxide ions and the evolution of gaseous oxygen on the surface:



One can see in the data shown in Fig. 4 that the shape of curves for compounds with $x = 0.05, 0.1$ is similar to the dependence $E-n$ for $\text{SrCo}_{0.8}\text{Fe}_{0.2}\text{O}_{3-z}$ ($0 < z < 0.5$) and differs only by the amount of transferred charge n (or intercalated oxygen, $z = n/2$). This is due to narrowing of the region of oxygen nonstoichiometry as a result of the introduction of highly charged Nb^{5+} ions and additional oxygen, to compensate for excessive positive charge, into the structure of $\text{SrCo}_{0.8}\text{Fe}_{0.2}\text{O}_{3-z}$. The occurrence of a plateau on the curves in the region of 200–250 mV and subsequent monotonous increase of the potential to 500–550 mV, corresponding to the evolution of gaseous oxygen on the working electrode, provide evidence that the change of oxygen stoichiometry from $\text{SrCo}_{0.8-x}\text{Fe}_{0.2}\text{Nb}_x\text{O}_{3-z}$ to $\text{SrCo}_{0.8-x}\text{Fe}_{0.2}\text{Nb}_x\text{O}_3$ involves the formation of intermediate products: at the first stage as a result of the two-phase reaction, then as a result of a monophasic reaction. For the oxidation of the samples with $x > 0.1$, the potential changes monotonously, therefore, oxidation proceeds in the single-phase

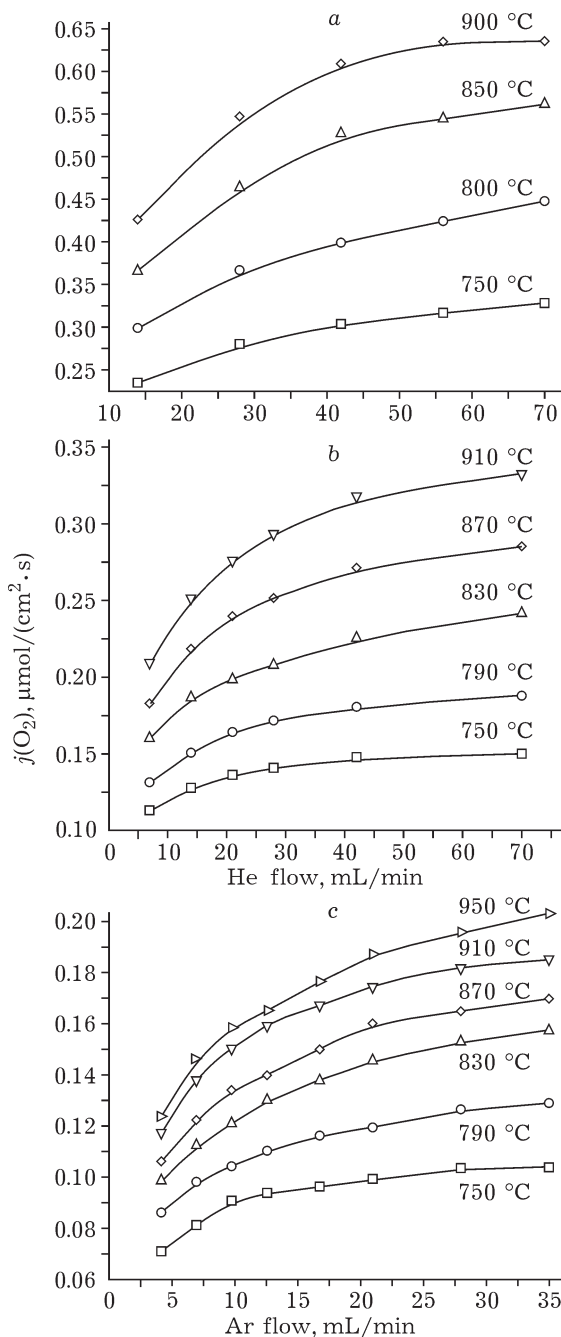


Fig. 5. Dependencies of oxygen fluxes through the membrane on the rate of blowing the inner side with the inert gas, for samples $\text{SrCo}_{0.75}\text{Fe}_{0.2}\text{Nb}_{0.05}\text{O}_{3-z}$ (a), $\text{SrCo}_{0.7}\text{Fe}_{0.2}\text{Nb}_{0.1}\text{O}_{3-z}$ (b), $\text{SrCo}_{0.6}\text{Fe}_{0.2}\text{Nb}_{0.2}\text{O}_{3-z}$ (c) at different temperatures.

mode through a continuous series of solid solutions with respect to oxygen. Using the data on the electrochemical oxidation, with the help of Cottrell equation, we can estimate the coefficient of the chemical diffusion of oxygen at room temperature [24]:

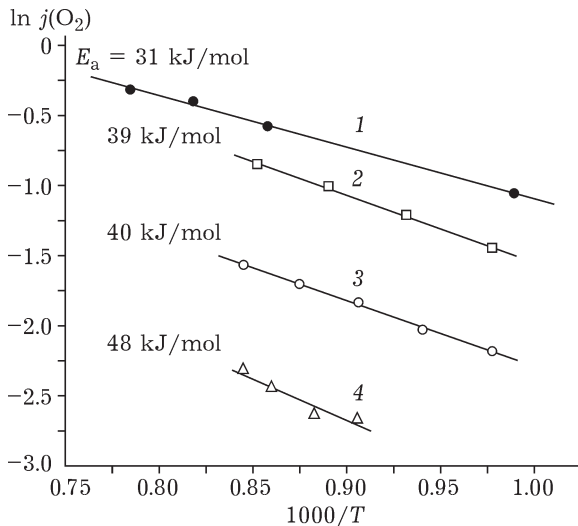


Fig. 6. Arrhenius plots of oxygen fluxes on reciprocal temperature for initial $\text{SrCo}_{0.8}\text{Fe}_{0.2}\text{O}_{3-z}$ sample and niobium-doped samples. The values of x : 0 (1), 0.05 (2), 0.1 (3), 0.2 (4).

$$t^{1/2} = \frac{nF(C - C_0)(\pi D)^{1/2}}{2j} \quad (4)$$

Substituting current density $j \sim 10^{-5}$ A/cm², the time of phase transition $t \sim 10^5$ s, change of oxygen concentration in the sample $(C - C_0) \sim 10^{-3}$ mol/cm³, we obtain diffusion coefficients within the range $(8 \cdot 10^{-9}) - (3 \cdot 10^{-10})$ cm²/s. It should be noted that the value 10^{-10} cm²/s at room temperature is extremely high for oxides. For example, extrapolation of high-temperature data for superionic oxide ZrO_2 stabilized with yttrium gives the value of oxygen diffusion coefficient at room temperature $\tilde{D} \sim 10^{-22}$ cm²/s [25].

An important functional characteristic of membrane materials is oxygen permeability at high temperature ($T > 700$ °C). The dependencies of oxygen fluxes through the membrane on the rate of blowing the inner side with the inert gas for the samples $\text{SrCo}_{0.75}\text{Fe}_{0.2}\text{Nb}_{0.05}\text{O}_{3-z}$, $\text{SrCo}_{0.7}\text{Fe}_{0.2}\text{Nb}_{0.1}\text{O}_{3-z}$, $\text{SrCo}_{0.6}\text{Fe}_{0.2}\text{Nb}_{0.2}\text{O}_{3-z}$ at different temperatures are shown in Fig. 5. With an increase in the rate of blowing with helium, the partial pressure of oxygen from the inner side of the membrane decreases. The gradient of the partial pressure of oxygen thus increases, which causes an increase in oxygen fluxes. Thus, oxygen fluxes reach 0.64, 0.33 and 0.16 mmol/(cm² · s) at 900 °C and inert gas flow 70 mL/min for $\text{SrCo}_{0.75}\text{Fe}_{0.2}\text{Nb}_{0.05}\text{O}_{3-z}$,

$\text{SrCo}_{0.7}\text{Fe}_{0.2}\text{Nb}_{0.1}\text{O}_{3-z}$, $\text{SrCo}_{0.6}\text{Fe}_{0.2}\text{Nb}_{0.2}\text{O}_{3-z}$, respectively. For comparison, the value of oxygen fluxes obtained by us for initial $\text{SrCo}_{0.8}\text{Fe}_{0.2}\text{O}_{3-z}$ is 0.8 mmol/(cm² · s) under the same conditions. The Arrhenius dependencies of oxygen fluxes on reciprocal temperature for the initial sample $\text{SrCo}_{0.8}\text{Fe}_{0.2}\text{O}_{3-z}$ and niobium-containing derivatives are shown in Fig. 6. One can see that doping with niobium causes a decrease in oxygen permeability but the activation energy of the process remains practically unchanged. This is likely to be connected with the fact that for non-isovalent doping of $\text{SrCo}_{0.8}\text{Fe}_{0.2}\text{O}_{2.5}$ with niobium (5+) compensation of excessive positive charge $\text{Nb}_{\text{Co}}^{\bullet}$ is accompanied both by the formation of strong NbO_6 octahedrons and by an increase in the coordination number of neighbouring cations in the B sublattice through the introduction of oxygen ions $\text{O}_i^{\prime\prime}$ into the lattice; they occupy the cavities of the brownmillerite structure – pseudo-interstices.

Dopant ions $\text{Nb}_{\text{Co}}^{\bullet}$ bound into strong NbO_6 octahedrons and mobile defects – pseudo-interstices $\text{O}_i^{\prime\prime}$ – are located in the second coordination sphere of Nb and screened by oxygen ions. This substantially lowers the trapping effect (strong Coulomb interaction between $\text{Nb}_{\text{Co}}^{\bullet}$ and $\text{O}_i^{\prime\prime}$), which, as a rule, brings an additional term E_i into the activation energy of oxygen transport ($E_a = E_m + E_i$). Insignificant decrease in oxygen fluxes with an increase in the concentration of dopant (Nb) can be connected with a decrease in the concentration of mobile oxide ions because a part of them gets bound through strong Nb–O bonds.

CONCLUSION

The synthesis of monophasic compounds having the composition $\text{SrCo}_{0.8-x}\text{Fe}_{0.2}\text{Nb}_x\text{O}_{3-z}$ ($0 \leq x \leq 0.4$) with perovskite structure was carried out. It was shown that highly charged Nb^{5+} cations isomorphically substitute cobalt cations in the B position of perovskite structure. The introduction of stable NbO_6 octahedrons into the lattice causes narrowing of the region of oxygen nonstoichiometry and suppresses the structural transition from perovskite to brownmillerite at low temperatures and partial pressures of oxygen.

Substituted perovskites $\text{SrCo}_{0.8-x}\text{Fe}_{0.2}\text{Nb}_x\text{O}_{3-z}$ ($0 \leq x \leq 0.2$) obtained in the work possess high oxygen mobility; the values of diffusion coefficients at room temperature are $8 \cdot 10^{-9}$ – $(3 \cdot 10^{-10}) \text{ cm}^2/\text{s}$. Oxygen fluxes through gas-tight membranes made of the materials under investigation were measured at high temperatures. The introduction of niobium causes insignificant decrease in oxygen permeability; however, the obtained values of oxygen fluxes are comparable with the data for the best oxygen conductors known at present.

Investigation gave evidence that perovskites having the composition $\text{SrCo}_{0.8-x}\text{Fe}_{0.2}\text{Nb}_x\text{O}_{3-z}$ ($0 \leq x \leq 0.2$) combine high transport properties and thermal stability. Due to this, they may be considered as promising materials for making oxygen-permeable membranes used for separation of atmospheric oxygen or partial oxidation of hydrocarbons in catalytic membrane reactors, as well as electrodes for solid oxide fuel elements.

REFERENCES

- 1 Sunarso J., Baumann S., Serra J. M., Meulenberg W. A., Liu S., Lin Y. S., Diniz da Costa J. C., *J. Membrane Sci.*, 320 (2008) 13.
- 2 Teraoka Y., Zhang H. M., Furukawa S., Yamazoe N., *Chem. Lett.*, 14, 11 (1985) 1743.
- 3 Bouwmeester H. J. M., Gellings P. J. Dense Ceramic Membranes for Oxygen Separation, *The CRC Handbook of Solid State Electrochemistry*, CRC Press, Enschede, 1996, pp. 482–542.
- 4 Liu L. M., Lee T. H., Qiu L., Yang Y. L., Jacobson A. J., *Mat. Res. Bull.*, 31, 1 (1996) 29.
- 5 Kharton V. V., Viskup A. P., Kovalevsky A. V., Jurado J. R., Naumovich E. N., Vecher A. A., Frade J. R., *Solid State Ionics*, 133 (2000) 57.
- 6 Waerenborgh J. C., Rojas D. P., Shaula A. L., Mather G. C., Patrakeeve M. V., Kharton V. V., Frade J. R., *Mater. Lett.*, 59 (2005) 1644.
- 7 Patrakeeve M. V., Markov A. A., Leonidov I. A., Kozhevnikov V. L., Kharton V. V., *Solid State Ionics*, 177 (2006) 1757.
- 8 Kharton V. V., Yaremchenko A. A., Valente A. A., Sobyanyin V. A., Belyaev V. D., Semin G. L., Veniaminov S. A., Tsipis E. V., Shaula A. L., Frade J. R., Rocha J., *Solid State Ionics*, 76 (2005) 781.
- 9 Patrakeeve M. V., Kharton V. V., Bakhteeva Yu. A., Shaula A. L., Leonidov I. A., Kozhevnikov V. L., Naumovich E. N., Yaremchenko A. A., Marques F. M. B., *Solid State Sci.*, 8 (2006) 476.
- 10 Savinskaya O. A., Nemudry A. P., Lyakhov N. Z., *Neorg. Mater.*, 43, 12 (2007) 1.
- 11 Savinskaya O. A., Nemudry A. P., Nadeev A. N., Tsybulya S. V., *Solid State Ionics*, 179 (2008) 1076.
- 12 Markov A. A., Leonidov I. A., Patrakeeve M. V., Kozhevnikov V. L., Savinskaya O. A., Ancharova U. V., Nemudry A. P., *Solid State Ionics*, 179 (2008) 1050.
- 13 Markov A. A., Savinskaya O. A., Patrakeeve M. V., Nemudry A. P., Leonidov I. A., Pavlyukhin Yu. T., Ishchenko A. V., Kozhevnikov V. L., *J. Solid State Chem.*, 182 (2009) 799.
- 14 Markov A. A., Patrakeeve M. V., Savinskaya O. A., Nemudry A. P., Leonidov I. A., Leonidova O. N., Kozhevnikov V. L., *Solid State Ionics*, 179 (2008) 99.
- 15 Daroukh M. Al, Vashook V. V., Ullmann H., Tietz F., Raj I. A., *Solid State Ionics*, 158 (2003) 141.
- 16 Nemudry A. P., Koroleva A. N., Pavlyukhin Yu. T., Podyacheva O. Yu., Ismagilov Z. R., *Izv. RAN. Ser. Fiz.*, 67, 7 (2003) 952.
- 17 Zhogin I. L., Nemudry A. P., Glyanenko P. V., Kamenetsky Yu. M., Bouwmeester H. J. M., Ismagilov Z. R., *Catal. Today*, 118 (2006) 151.
- 18 Aleksandrov K. S., Beznosikov B. V., *Perovskitopodobnye Kristally*, Nauka, Novosibirsk, 1997.
- 19 Nemudry A., Uvarov N., *Solid State Ionics*, 177 (2006) 2491.
- 20 Vul D. A., Salje E. K. H., *Physica C*, 253 (1995) 231.
- 21 Savytskii D. I., Trots D. M., Vasylechko L. O., Tamura N., Berkowski M., *J. Appl. Cryst.*, 36 (2003) 1197.
- 22 Nemudry A., Rudolf P., Schoellhorn R., *Chem. Mater.*, 8 (1996) 2232.
- 23 ten Elshof J. E., Bouwmeester H. J. M., Verweij H., *Appl. Catal. A: Gen.*, 130 (1995) 195.
- 24 Jiang S. P., Love J. G., Badwal S. P. S., *Key Eng. Mater.*, 125–126 (1997) 81.
- 25 Nemudry A., Goldberg E. L., Aguirre M., Alario-Franco M. A., *Solid State Sci.*, 4 (2002) 677.